THE JOURNAL OF PHYSICAL CHEMISTRY B

pubs.acs.org/JPCB Article

Geometry and Flexibility of Optimal Catalysts in a Minimal Elastic Model

Olivier Rivoire*

Cite This: J. Phys. Chem. B 2020, 124, 807−813 Read Online

ACCESS | Metrics & More | Article Recommendations | Supporting Information

ABSTRACT: We have general knowledge of the principles by which catalysts accelerate the rate of chemical reactions but no precise understanding of the geometrical and physical constraints to which their design is subject. To analyze these constraints, we introduce a minimal model of catalysis based on elastic networks where the implications of the geometry and flexibility of a catalyst can be studied systematically. The model demonstrates the relevance and limitations of the principle of transition-state stabilization: optimal catalysts are found to have a geometry complementary to the transition state but a degree of flexibility that nontrivially depends on the parameters of the reaction as well as on external parameters such as the concentrations of reactants and products. The results illustrate how simple physical models can provide valuable insights into the design of catalysts.

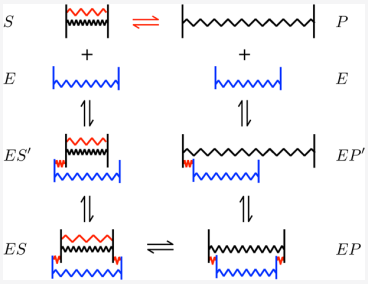

INTRODUCTION

Catalysts, which increase the rate of chemical reactions without being part of their products, are essential to biological processes as well as to the industrial production of most chemicals. We have a general theory of catalysis, transition-state theory,[1,2] and detailed knowledge of the mechanisms by which many catalysts operate, in particular enzymes.[3] We also have an increasing capacity to model and numerically simulate catalytic processes at an atomic level.[4] Yet, basic questions pertaining to the existence of fundamental geometrical and physical constraints to catalysis are still the object of speculations: To what extent does efficient catalysis require catalysts to be rigid?[5] Or thermally stable?[6] Does it impose a minimal size on catalysts?[7] Is catalysis subject to a general rate−accuracy trade-off?[8]

Answers to such questions would help us uncover the design principles of natural enzymes,[9] direct the experimental evolution of novel enzymes,[10] and clarify the conditions under which life can emerge.[11]

Missing is a theoretical framework that is sufficiently elaborate to account for geometric and physical constraints yet sufficiently simple to allow for a systematic comparison of varied geometries and physical designs. For this purpose, the low-dimensional phase-space formulation of transition-state theory is too abstract as it does not refer explicitly to the spatial architecture of catalysts. The atom-level description of models studied by molecular dynamic simulations is, on the other hand, too detailed as it prohibits computational exploration of a large number of architectures.

An alternative lies in the simplified physical models developed to study properties of proteins other than catalysis, notably folding,[12] binding,[13] and allostery.[14] Particularly insightful are elastic network models, which approximate molecules by a network of beads interacting through elastic springs.[15] In their different guises, these models have provided conceptual and quantitative insights into several features of proteins, including thermal fluctuations,[16] conformational changes,[17] unfolding kinetics,[18,19] specificity,[20,34] and allostery.[21,22]

Here, we propose to adapt the framework of elastic network models to study catalysis. We illustrate this proposal by defining and solving a one-dimensional model of catalysis. Our model may be viewed as a reformulation and systematic analysis of a model of strain-induced catalysis first suggested by Haldane[23] and later partly formalized by Gavish.[24−26] While deliberately minimal, the model addresses a key design challenge: an efficient catalyst must stabilize the transition state of the reaction to accelerate it but also bind to the reactant and release the product. These conflicting demands lead to nontrivial constraints on flexibility, which our model recapitulates. The model also demonstrates how the optimal design of a catalyst depends, beyond the mechanisms of the reaction, on the conditions under which catalysis occurs. Our analysis is limited to one dimension, but the model is straightforward to extend, if not to solve, in two or three dimensions. Our approach thus complements other bottom-up studies of catalysis[24,27] toward a better understanding of the geometrical and physical constraints to which proficient catalysts are subject.

Received: January 10, 2020
Published: January 28, 2020

https://dx.doi.org/10.1021/acs.jpcb.0c00244
J. Phys. Chem. B 2020, 124, 807−813

METHODS

Analyzing the physical and geometrical constraints to efficient catalysis requires a physical model that specifies the range of designs to be examined and a criterion to quantify catalytic efficiency. Our choices in defining such a model are guided by a principle of simplicity, the goal being to obtain a physically coherent framework where a large number of different architectures can effectively be explored and compared.

Physical Model. Elastic network models are one of the simplest physical models where geometry, strain, and energy can be related. They consist of beads interacting through elastic springs and have been extensively used to study the internal motions of proteins.[15] Each spring is characterized by two parameters, a spring constant and a free length. Varying the number of beads and the parameters of the springs that connect them allows for the sampling of a large number of designs, including networks approximating three-dimensional protein structures.[15] Here, we propose to describe not only a catalyst but also its substrate and their interaction within a common elastic network model. To this end, we assume that each spring has a maximal extension above which it breaks and below which it reforms. More precisely, each spring contributes to the total energy by $k(|x|-l)^2/2 - k(z-l)^2/2$ if the extension x satisfies $|x| < z$ and 0 if $|x| > z$, where $k > 0$ is the spring constant, $l > 0$ is the free length, and $z > l$ is the maximal extension. When the beads are subject to Brownian motion, which accounts for their interaction with a solvent, bonds may thus break or form as a result of thermal fluctuations.

The rupture of a bond between two beads defines an elementary chemical reaction. To have a single product as well as a single reactant, we consider a case where this rupture does not compromise the connectivity of the substrate. This is achieved by assuming that a second unbreakable bond (with infinite maximal extension) links the two beads: the presence of the two springs then defines the reactant S while the absence of the breakable spring defines the product P (Figure 1, top line).

In this framework, the simplest catalyst also consists of just two beads joined by a single unbreakable spring. To describe its interaction with the substrate, either in the form of the reactant S or the product P, we assume that each bead of the catalyst can interact through a breakable spring with one, and only one, of the beads of the substrate (Figure 1).

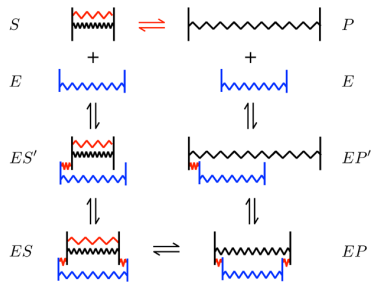

Figure 1. Elastic network model of catalysis. The reaction $S \rightleftharpoons P$ is defined on the top. The reactant S consists of two beads connected by two springs (here represented by vertical lines). One spring (in red) breaks when its extension exceeds a threshold, which results in the product P. The system is subject to thermal fluctuations, and the reaction may thus occur spontaneously. A catalyst E (in blue) similarly consists of two beads connected by a spring. Each bead of the catalyst can interact with one bead of the substrate through a breakable spring (in red) that forms when the distance between the two beads is below a threshold and breaks when their distance is above this same threshold. Six nonequivalent states can be distinguished, $S + E$, ES', ES, EP, EP', and $P + E$, depending on whether each type of breakable spring is broken or not.

In total, our elastic network model thus comprises four beads and five springs, three of which being effectively absent if their extension exceeds a given threshold. Assuming the breakable springs to have a vanishing free length, the model is then specified by eight parameters (Table 1).

Table 1. Eight Parameters of the Elastic Network Model[a]

parameter	spring constant	free length	maximal extension
substrate scissile bond	k_a	0	z_a
substrate non-scissile bond	k_r	l_r	∞
catalyst internal bond	k_e	l_e	∞
substrate−catalyst interaction	k_i	0	z_i

[a]Each bond has three parameters: a spring constant k, a free length l that defines an elastic interaction and a maximal extension $z > l$ beyond which this interaction is no longer present. The substrate consists of two beads connected by two bonds, one scissile ($z_a < \infty$) and the other not ($z_r = \infty$). The catalyst consists of two beads connected by a single bond. The interaction between the beads of the substrate and those of the substrate is described by breakable springs. The free lengths of breakable springs are taken to be zero.

Criteria for Catalytic Efficiency. There is no intrinsically optimal catalyst. Depending on the setup, and not just the reaction to be catalyzed, different criteria are relevant to scoring catalytic activity. Optimizing these different criteria generally leads to different optimal designs.

Consider for instance a measure of catalytic efficiency commonly adopted in enzymology, the ratio k^+_{cat}/K^+_M. It assumes that the rate $v = \partial p/\partial t$ at which the concentration of products p increases depends on the concentration of reactants s and on the total concentration e_0 of catalysts by the Michaelis−Menten equation,[28]

$$v = \frac{k^+_{cat} e_0 s}{K^+_M + s}. \tag{1}$$

The ratio k^+_{cat}/K^+_M then characterizes the initial rate of the reaction, when $s \ll K^+_M$. In general, however, eq 1 indicates that the rate v depends on the concentration s of reactants. The ratio k^+_{cat}/K^+_M should indeed be generally interpreted as a measure of specificity rather than a measure of catalytic efficiency.[29]

To see how optimizing k^+_{cat}/K^+_M may lead to unphysical results, consider the simplest case where eq 1 arises, under the scheme $E + S \underset{k_{-1}}{\overset{k_1}{\rightleftharpoons}} ES \xrightarrow{k_2} E + P$ where the complex ES is assumed to be in a quasi-steady state.[28] In this case, $k^+_{cat} = k_2$ and $k^+_M = (k_{-1} + k_2)/k_1$. Taking $k_{-1} = 0$, we obtain $k^+_{cat}/K^+_M = k_1$, which is independent of k_2. Formally, k^+_{cat}/K^+_M can thus be made arbitrarily large by minimizing k_{-1} and maximizing k_1, irrespective of k_2, even though k_2 controls an essential step and $k_2 = 0$ means that no catalysis takes place. The catch is in the assumption $s \ll K^+_M$, which underlies the choice of the ratio k^+_{cat}/K^+_M as a measure of catalytic efficiency. When $k_{-1} = 0$, this assumption implies $s \ll k_2/k_1$, which depends on k_2 and is certainly not satisfied when $k_2 = 0$. This simple example illustrates the need to consider explicitly the concentration s of reactants to obtain physically meaningful results.[a] As a corollary,

https://dx.doi.org/10.1021/acs.jpcb.0c00244
J. Phys. Chem. B 2020, 124, 807−813

a family of optimal designs is defined, which depend on the concentration s of reactants and not just on the mechanisms of the reaction. More generally, optimal designs also depend on the concentration p of products, which is assumed to be $p = 0$ in eq 1.

Here, we choose to treat the concentrations of reactants s and products p as two fixed parameters and to score catalytic activity by the rate $v = \partial p/\partial t$ at which the product is formed. This assumes a reservoir of reactants and products so that their concentrations are constant despite the reactions that consume or produce them. This is, however, not the only possible choice. One may alternatively consider a closed system with an initial concentration of reactants and score the concentration of products after a fixed time, or consider a chemostat with a fixed in-flow of reactants and catalysts, a fixed dilution rate and score the out-flow of products.

Solvable One-Dimensional Model. The model presented in Figure 1 is defined in any dimension. We study it here in one dimension where it has only three independent internal degrees of freedom and can be solved analytically. The details of this solution are presented in the Supporting Information, and we focus below on the results and assumptions on which they rely. While these assumptions constrain the range of examined designs, they are justified a posteriori by the finding of locally optimal designs within their range of validity.

Uncatalyzed Reaction. In one dimension, a substrate is characterized by a single internal degree of freedom, the distance x_0 between its two beads, and five physical parameters, the spring constants k_a and k_r of the two springs that connect the two beads, their free lengths l_a and l_r, and the maximal extension z_a of the breakable spring (a stands for "attractive" and r for "repulsive"). Without loss of generality, we assume $l_a = 0$ (Table 1). The number of parameters can be further reduced to two by considering adimensional quantities (Supporting Information, Section IA).

As long as the distance x_0 between the two beads satisfies $|x_0| < z_a$, the two springs are present and equivalent to a single spring with effective parameters

$$k_{ar} = k_a + k_r, \qquad l_{ar} = \frac{k_r l_r}{k_a + k_r} \tag{2}$$

We assume $0 < l_{ar} < z_a < 2l_{ar}$ so that a substrate with initial extension $x_0 = l_{ar}$ is more likely to break ($x_0 > z_a$) than to invert the relative position of its two beads ($x_0 < 0$); in this approximation, the interaction potential between the beads is harmonic (Supporting Information, Section IA). For the reactant and the product to be stable, the equilibrium distance with and without the scissile bond must be below and beyond the breaking point, respectively, which imposes $l_{ar} < z_a < l_r$. Additionally, we choose parameters so that the state with a broken bond is the lowest energy state (Supporting Information, Section IA and Figure 2).

We compute the rates of transition between states using Kramers' escape formula,[30] which assumes that the time scales of relaxation within each state are much smaller than the transition rates. This is valid provided barrier heights are large compared to $k_B T$ where T is the temperature and k_B is Boltzmann's constant (Supporting Information, Section IB). This leads to the forward and reverse rates ρ_u^+ (for $S \to P$) and ρ_u^- (for $P \to S$) given by

$$\rho_u^+ = \sqrt{k_{ar}}\, e^{\beta k_{ar}(z_a - l_{ar})^2/2}$$
$$\rho_u^- = \sqrt{k_r}\, e^{\beta k_r (z_a - l_r)^2/2} \tag{3}$$

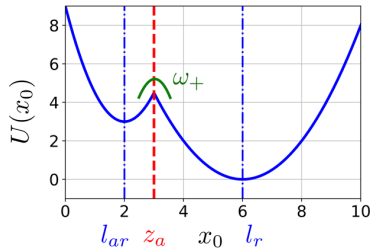

Figure 2. Potential for the uncatalyzed reaction $S \rightleftharpoons P$. The potential $U(x_0)$ is a function of the extension x_0 of the substrate. The two states S and P are defined by $x_0 < z_a$ and $x_0 > z_a$, respectively, with the transition between the two defining the reaction $S \rightleftharpoons P$. The parameters (Table 1) for this graph are $k_a = 2$, $z_a = 3$, $l_r = 6$, $k_r = 1$. When computing escape rates, we assume a smooth curvature ω_+ at the transition state $x_0 = z_a$, where the value of ω_+ is fixed independently of the other parameters (Supporting Information, Section IB).

where $\beta = k_B T^{-1}$. In these formulae, the unit of time is chosen so that the viscosity γ of the solvent and the curvature ω_+ of the potential at the barrier do not appear explicitly (Supporting Information, Section IB). Given these rates, the reaction $S \to P$ is thermodynamically favored provided $p/s < K_{eq}$ where s and p are the concentrations of the reactant S and product P and where $K_{eq} = \rho_u^+/\rho_u^-$ is the equilibrium constant of the reaction.

In what follows, we consider as parameters of the reaction (Table 1) the values $k_a = 2$, $z_a = 3$, $l_r = 6$, $k_r = 1$, and $\beta = 2$ so that $l_{ar} = 2$ and $k_{ar} = 3$ in eq 2. These values, which satisfy the different assumptions that we make (Figure S1), correspond to the potential shown in Figure 2.

Catalysis. The catalyst is characterized by the spring constant k_e and free length l_e of the unbreakable spring that connects its two beads (Figure 1). Each of these beads can interact with only one bead of the substrate, and the two interactions are described by equivalent breakable springs with spring constant k_i, free length $l_i = 0$, and maximal extension z_i (Table 1). We assume that the catalyst is rigid enough to maintain the relative position of its beads ($k_B T \ll k_e l_e^2/2$, Supporting Information, Section IC).

The system formed by the catalyst and the substrate can possibly be in 2^3 states, depending on whether each of the three scissile bonds is broken or not. Given the equivalence between the two bonds by which the substrate and the catalyst interact, these eight states define six physically distinct states (Supporting Information, Section ID and Figure 1). These physical states are well-defined if they are associated with local minima of the potential, and we consider parameters for which this is the case (Supporting Information, Section ID).

When all six states are well-defined, the catalysis is the result of the series of reactions

$$E + S \underset{\rho_1^-}{\overset{\rho_0^+}{\rightleftharpoons}} ES' \underset{\rho_2^-}{\overset{\rho_1^+}{\rightleftharpoons}} ES \underset{\rho_3^-}{\overset{\rho_2^+}{\rightleftharpoons}} EP \underset{\rho_4^-}{\overset{\rho_3^+}{\rightleftharpoons}} EP' \underset{\rho_5^-}{\overset{\rho_4^+}{\rightleftharpoons}} E + P \tag{4}$$

where the intermediate states ES', ES, EP, EP' are illustrated in Figure 1. The transitions $ES' \rightleftharpoons EP'$ are ignored, which is justified when the rates $\rho_u^\pm$ of the uncatalyzed reaction are negligible compared to the rates of the catalyzed reaction, that is, $\rho_1^+ \gg \rho_u^+$ and $\rho_4^- \gg \rho_u^-$. We assume $\rho_0^+ = 1$ and $\rho_5^- = 1$[b] and obtain the other rates by application of Kramers' escape formula (Supporting Information, Section IE).

Under the assumptions that the concentrations e_0 of catalysts (under their different forms), s of reactants, and p of products are maintained constant and that the concentrations of all

https://dx.doi.org/10.1021/acs.jpcb.0c00244
J. Phys. Chem. B 2020, 124, 807−813

intermediates are at the steady state, the rate $v = \partial p/\partial t$ of product formation takes the form (Supporting Information, Section IF)

$$\frac{v}{e_0} = \frac{k_{cat}^{+} s/K_M^{+} - k_{cat}^{-} p/K_M^{-}}{1 + s/K_M^{+} + p/K_M^{-}} \quad (5)$$

The parameters of this reversible Michaelis−Menten equation[28] depend on the eight spring parameters given in Table 1 via the rates in eq 4. They also depend on the temperature of the solvent but not on its viscosity, nor on the curvature of the potential near the activation barriers, which we assume to be identical for all barriers (Supporting Information, Section IB).

RESULTS

To characterize optimal designs within the model, we maximize the reaction rate v over the four parameters of the catalyst: k_e, l_e, which characterize its flexibility and geometry, and k_i, z_i, which characterize the strength and range of its interaction with the substrate (Table 1). The optimum generally depends on the four physical parameters of the substrate, k_a, z_a, k_r, l_r (Table 1), on the concentrations s, p at which the reactant S and product P are present, and on the temperature T of the solvent, represented by $\beta = 1/(k_B T)$.

For the substrate, we consider the parameters of Figure 2 $k_a = 2$, $z_a = 3$, $k_r = 1$, $l_r = 6$, which correspond to parameters $k_{ar} = 3$ and $l_{ar} = 2$ for the effective bond of the reactant (eq 2). For the medium, we first consider the parameters $s = 10^{-1}$, $p = 0$, and $\beta = 2$. With these values, we find a locally optimal design (Figure S2) that satisfies all the assumptions involved in the derivation of the rate v : $\hat{k}_e = \infty$, $\hat{l}_e = 3$, $\hat{k}_i \approx 13$, $\hat{z}_i = 0.5$.

This solution is consistent with the proposal that an optimal catalyst must stabilize the transition state of the reaction:[31,32] the catalyst is maximally rigid ($\hat{k}_e = \infty$) with a length that matches that of the transition state ($\hat{l}_e = z_a$). Additionally, the range of interaction $\hat{z}_i$ is adapted to the free length of the substrate: $\hat{l}_e - 2\hat{z}_i = l_{ar}$. The value of the optimal interaction strength $\hat{k}_i$ is, on the other hand, less obvious to interpret. It takes a finite value, contrary to what a naïve application of the principle of transition-state stabilization would predict. The optimal value of k_i represents indeed a trade-off between the need to stabilize the transition state, which requires rigidity, and the need to release the product, which requires flexibility (Figure 3). The energy landscape associated with this optimal design can be represented in two dimensions as a rigid catalyst with $\hat{k}_e = \infty$ leaves only two independent internal degrees of freedom (Figure 4).

Varying the different parameters around the above values, we verify that the relationships associated with transition-state stabilization,

$$\hat{k}_e = \infty, \quad \hat{l}_e = z_a, \quad \hat{z}_i = \frac{z_a - l_{ar}}{2} \quad (6)$$

are always nearly satisfied, while $\hat{k}$ is, on the other hand, parameter-dependent (Figures S3 and S4). We analyze in what follows the determinants of the optimal interaction strength $\hat{k}_i$ assuming that the other parameters of the catalyst are given by eq 6.

Dependence on Concentrations. Varying the concentration s of reactants at vanishing concentration of products ($p = 0$), we find that k_i has a nontrivial maximum $\hat{k}_i$ that decreases with s (Figure 5). In particular, in the limit $s \to 0$ where the problem is equivalent to optimizing the specificity constant k_{cat}^{+}/K_M^{+}, we have $\hat{k}_i \to \infty$: the strength of the interaction between the substrate and catalyst becomes infinite. This result illustrates how optimizing the ratio k_{cat}^{+}/K_M^{+} can lead to unphysical designs

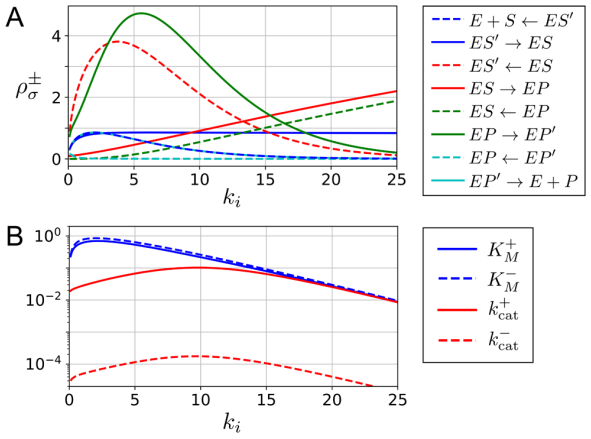

Figure 3. (A) Rates $\rho_\sigma^{\pm}$ for the series of transitions given in eq 4 as a function of the flexibility k_i of the interaction between substrates and catalysts. As k_i increases, the rate ρ_2^{+} of forward catalysis $ES \rightarrow EP$ increases (full red line), along with the rate ρ_3^{-} of reverse catalysis $ES \leftarrow EP$ (dotted green line), but the rates of product release $EP \rightarrow EP'$ (full green line) and $EP' \rightarrow E + P$ (full cyan line behind the blue dotted line) decrease. (B) Michaelis−Menten parameters defined by eq 5. Each parameter has a maximum for an intermediate value of k_i. In these graphs, the parameters of the substrate are as in Figure 2 and those of the catalyst other than k_i are given by Eq. 6. Note that the rates are not independent but satisfy $\prod_\sigma \rho_\sigma^{+}/\prod_\sigma \rho_\sigma^{-} = (k_{cat}^{+} K_M^{-})/(K_M^{+} k_{cat}^{-}) = K_{eq}$ where K_{eq} is the equilibrium constant of the uncatalyzed reaction (Haldane relationship).

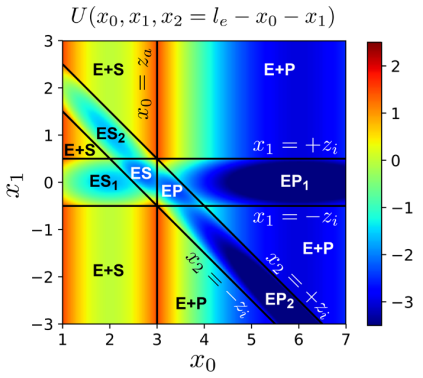

Figure 4. Energy landscape of a substrate−catalyst system for an optimal catalyst with infinite rigidity. The two degrees of freedom are the distance x_0 between the two beads of the substrate (the reaction coordinate) and the relative position x_1 between a bead of the catalyst and the bead of the substrate with which it interacts. The relative position x_2 between the other bead of the catalyst and the other bead of the substrate is given by $x_2 = \hat{l}_e - x_0 - x_1$ where $\hat{l}_e$ is the fixed length of the rigid catalyst. The different states are separated by black lines corresponding to the thresholds beyond which one of the three scissile bonds of the model ruptures: $x_0 = z_a$, $x_1 = \pm z_i$ and $x_2 = \pm z_i$. Here, we distinguish between the two states ES_1, ES_2 and EP_1, EP_2 instead of subsuming them under common states ES' and EP'. The parameters are as in Figure 3 with $k_i = 13$, and the reference $U = 0$ is taken to corresponds to the minimal energy of the state $E + S$.

https://dx.doi.org/10.1021/acs.jpcb.0c00244
J. Phys. Chem. B 2020, 124, 807−813

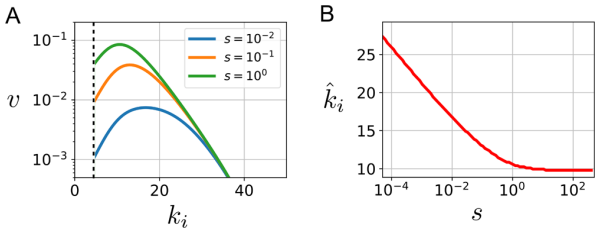

Figure 5. (A) Reaction rate v for the catalyzed reaction as a function of the interaction strength k_i for three different concentrations s of the reactant (and no product, $p = 0$), showing that the optimal value of k_i depends on s. For k_i smaller than the dashed vertical line, the state EP is unstable and the reaction does not follow the scheme of eq 4. (B) Optimal interaction strength $\hat{k}_i$ as a function of s.

as, in this limit, a catalyst is unable to release its product (Figure 3).

A non-zero concentration of products ($p \neq 0$) introduces an additional constraint, product inhibition. For catalysis to take place, p should be small enough for the reaction to be thermodynamically favored: $p/s<K_{eq}$ where $K_{eq} = \rho_u^+/\rho_u^-$ is the equilibrium constant of the uncatalyzed reaction $S \underset{\rho_u^-}{\overset{\rho_u^+}{\rightleftharpoons}} P$. Under this condition, we find that $\hat{k}_i$ is a decreasing function of both s and p (Figure 6).

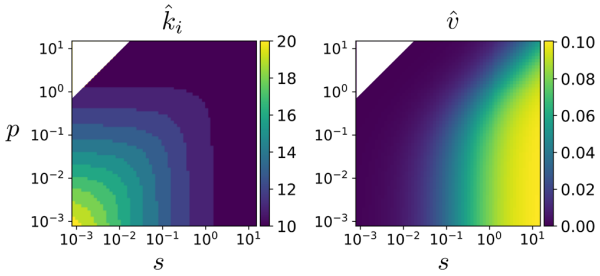

Figure 6. Optimal values of the interaction strength $\hat{k}_i$ and optimal reaction rate $\hat{v}$ as a function of the concentration s of reactants and p of products. The white triangle in the upper left corner corresponds to $p/s>K_{eq}$ where K_{eq} is the equilibrium constant of the uncatalyzed reaction $S \rightleftharpoons P$ in which case the reaction rate v cannot possibly be positive.

Dependence on Physical Parameters. The dependence of $\hat{k}_i$ on the physical parameters of the substrate k_a, z_a, k_r, l_r (Table 1) is shown in Figure 7. The results are at first sight counterintuitive. When increasing k_a, for instance, the activation barrier becomes higher but the interaction strength $\hat{k}_i$ of the optimal catalyst becomes weaker. Similarly, increasing z_a increases the activation barrier but is again associated with a smaller $\hat{k}_i$. On the other hand, substrates with increased k_r or l_r have a lower activation barrier but are associated with a larger $\hat{k}_i$.

To rationalize these results, note that varying k_a, z_a, k_r, or l_r implies not only a different optimal interaction strength $\hat{k}_i$ but, from Eq. 6, a different optimal extension $\hat{l}_e = z_a$ and a different optimal interaction range $\hat{z}_i = (z_a - l_{ar})/2$ (Figures S2 and S3). If instead of considering

$$\hat{k}_i(k_a) = \arg\max_{k_i} v(z_i = (z_a - l_{ar})/2, k_a) \quad (7)$$

where l_{ar} depends on k_a (eq 2), as in the red curve of the first panel of Figure 7, we consider

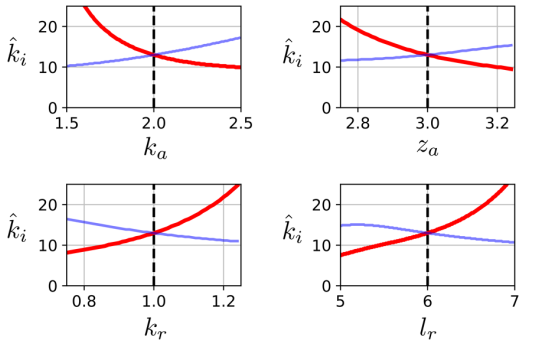

Figure 7. Optimal interaction strength $\hat{k}_i$ (in red) as a function of the physical parameters of the substrate, the strength k_a of the scissile bond, its maximal extension z_a, the strength k_r of the non-scissile bond, and its extension l_r (Table 1). When varying a parameter of the substrate, all the optimal parameters of the catalyst, and not only $\hat{k}_i$, generally take different values. If fixing these other variables and optimizing over $\hat{k}_i$ only as in eq 8 is performed, one obtains the blue curves that show opposite trends. The top graphs can also be related to the bottom graphs by noticing that the problem depends on the parameters k_a, z_a, k_r, and l_r through the dimensionless quantities k_a/k_r and l_r/z_a (eq 8).

$$\tilde{k}_i(k_a) = \arg\max_{k_i} v(z_i, k_a) \quad (8)$$

where z_i is fixed, we obtain the blue curve, which is an increasing function of k_a. Mathematically, the observation that stronger bonds are best broken by catalysts making weaker interactions with their substrate is thus explained by the difference between optimizing over a single variable versus optimizing over all variables jointly. Physically, a stronger k_a reduces the equilibrium length l_{ar} of the reactant and the catalyst needs to be more flexible to bind both to this smaller reactant and to the transition state whose location z_a is unchanged. Reasoning on just one parameter may thus be misleading because varying this parameter may have an incidence on multiple steps of the catalytic cycle and some of these effects may be compensated for by varying other parameters. Mutatis mutandis, similar arguments explain the nontrivial dependence on the other parameters shown in Figure 7.

DISCUSSION AND CONCLUSIONS

We introduced a simple but general elastic network framework for studying the geometrical and physical constraints to which efficient catalysts are subject and illustrated it with the analytical solution of an elementary one-dimensional model.

The solution demonstrates the relevance and limitations of the principle of transition-state stabilization, which reduces catalysis to binding to (analogues of) the transition state of the reaction.[31,32] While we find that the geometry of optimal catalysts matches the geometry of the transition state, consistent with this principle, we also find that binding to this state should not be maximized. Instead, some flexibility is needed to bind to the reactant and release the product in addition to stabilizing the transition state. The additional constraints that these requirements impose might explain why catalytic antibodies selected for transition-state stabilization with no consideration of product release are only modest catalysts.[33]

Binding to the reactant less than to the transition state but more than to the product, which are all chemically similar, poses a problem of fine discrimination. As previously proposed,[34] physical solutions to such problems can rely on a conformational

https://dx.doi.org/10.1021/acs.jpcb.0c00244
J. Phys. Chem. B 2020, 124, 807−813

switch: this is the case in the present model where the relative positions of the beads of the catalyst and the substrate are swapped during the transition $ES \rightleftharpoons EP$ (Figure 1).

While the model is not meant to make quantitative predictions, we note that the optimal strength of interaction between the substrate and catalyst is systematically larger than the strength of the bond to break; for instance, in Figure 3B, k^+_{cat} is maximal for $\hat{k}_i \approx 5$. This is in contrast to enzymes, which can catalyze the rupture of covalent bonds by means of weaker noncovalent interactions. Introducing physical limitations on the strength and length of the various bonds may thus contribute to explaining why enzymes are so large[7] and why they make multiple interactions with their substrate. This line of reasoning was first followed by Gavish who estimated how much stress an enzyme can exert on a substrate based on a similar toy model;[25] his analysis, however, does not consider the full catalytic cycle and, in particular, the need for the catalyst to be flexible to release the product. Besides physical limitations, evolutionary limitations, in particular the granularity of the sequence space, may also be relevant to these questions.[34]

Our model captures another feature of catalysis that is likely to be very general: efficient catalysts are not only optimized for the reaction but for the conditions under which catalysis occurs. In the model, these conditions include the temperature and the concentrations of reactants and products on which the optimal degree of flexibility $\hat{k}_i$ depends. In another setup, these concentrations may not be maintained constant and other parameters may be relevant, such as the concentration of catalysts or the fluctuations due to low concentrations of reactants.[35]

At a physical level, approximating a molecule by an elastic network is obviously an extreme oversimplification. Enzymes, in particular, are arguably not purely mechanical devices but as importantly electronic devices. Harmonic potentials may describe small distortions of charge distributions as well as mechanical strain, but their particular form, as our simple treatment of the solvent[36] or our omission of quantum effects,[37] certainly limit us to a subset of possible designs.

Within our mechanical framework, several extensions of the model may, however, already be of interest. First, our solution applies only under a number of assumptions that guarantee a sequence of transitions, each described by Kramers' theory.[30] We showed that a locally optimal solution exists within the range of validity of these assumptions but did not exclude other solutions beyond this range. Several additional constraints that are relevant to enzymes would also be interesting to incorporate, such as constraints on specificity for the substrate[3] or long-term evolutionary constraints.[38]

Irrespective of new constraints, a primary challenge is to extend the analysis beyond the four-node elastic network in one dimension that we solved in this work. The analysis of larger systems faces two computational difficulties: computing rates of reaction for networks involving many physical degrees of freedom and optimizing over the architecture and parameters of a large number of networks. The first difficulty may be tackled through molecular dynamics simulations from which rates of reactions can be estimated. The second difficulty is also limiting the evolution of natural enzymes, which nevertheless include very efficient catalysts, and could therefore be overcome by taking an evolutionary approach. Extending our analysis to larger networks in higher dimensions is necessary to capture features absent from our minimal model but likely to be essential to actual catalysts: beyond one dimension, applying a sufficient strain is for instance no longer sufficient and orienting this strain becomes a significant issue; for large networks, entropic effects may also play a predominant role. Finally, efficient catalysis might be achieved by more than one design when considering large systems; alternative designs might then differ in interesting ways, for example, in their capacity to adapt through small modifications to new catalytic demands.

■ ASSOCIATED CONTENT

Supporting Information

The Supporting Information is available free of charge at https://pubs.acs.org/doi/10.1021/acs.jpcb.0c00244.

Details of calculations, including Tables S1−S4 summarizing the definitions of the different states; Figure S1: graphical representation of the range of parameters for which the assumptions made on the spontaneous reaction are valid; Figure S2: dependence of the rate v of product formation on the different parameters of the catalyst; Figure S3: dependence of the optimal parameters $\hat{k}_i$ on the external parameters s, p, and β; Figure S4: dependence of the optimal parameters $\hat{k}_i$ on the physical parameters of the substrate k_a, z_a, k_r, and l_r (PDF)

■ AUTHOR INFORMATION

Corresponding Author

Olivier Rivoire − *Center for Interdisciplinary Research in Biology (CIRB), Collège de France, CNRS, INSERM, PSL Research University 75005 Paris, France;* orcid.org/0000-0002-1820-1324; Email: olivier.rivoire@college-de-france.fr

Complete contact information is available at: https://pubs.acs.org/10.1021/acs.jpcb.0c00244

Notes

The author declares no competing financial interest.

■ ACKNOWLEDGMENTS

This work benefited from stimulating discussions with Clément Nizak and Zorana Zeravcic and from comments by Eric Rouviere.

■ ADDITIONAL NOTES

[a]One could also ignore K^+_M and score catalytic efficiency by k^+_{cat} but this choice would not account for the rate at which the product is generated.

[b]We can always redefine the concentrations s and p so that it is the case. When optimizing at given values of s and p, however, this rescaling matters. A nonequivalent choice would for instance be to take $\rho^+_0 = \rho^-_S = 4z_i$ with $4z_i$ representing the "cross section" for the collision between catalysts and substrates.

■ REFERENCES

(1) Eyring, H. The activated complex in chemical reactions. *J. Chem. Phys* **1935**, *3*, 107−115.

(2) Evans, M. G.; Polanyi, M. Some applications of the transition state method to the calculation of reaction velocities, especially in solution. *Trans. Faraday Soc.* **1935**, *31*, 875.

(3) Fersht, A. *Structure and mechanism in protein science: a guide to enzyme catalysis and protein folding*; Macmillan: 1999.

(4) Karplus, M.; McCammon, J. A. Molecular dynamics simulations of biomolecules. *Nat. Struct. Mol. Biol.* **2002**, *9*, 646−652.

(5) Kraut, J. How do enzymes work? *Science* **1988**, *242*, 533−540.

(6) Karshikoff, A.; Nilsson, L.; Ladenstein, R. Rigidity versus flexibility: the dilemma of understanding protein thermal stability. *FEBS J.* **2015**, *282*, 3899−3917.
(7) Srere, P. A. Why are enzymes so big? *Trends Biochem. Sci.* **1984**, *9*, 387−390.
(8) Tawfik, D. S. Accuracy-rate tradeoffs: how do enzymes meet demands of selectivity and catalytic efficiency? *Curr. Opin. Chem. Biol.* **2014**, *21*, 73−80.
(9) Davidi, D.; Longo, L. M.; Jabłońska, J.; Milo, R.; Tawfik, D. S. A bird's-eye view of enzyme evolution: chemical, physicochemical, and physiological considerations. *Chem. Rev* **2018**, *118*, 8786−8797.
(10) Goldsmith, M.; Tawfik, D. S. Directed enzyme evolution: beyond the low-hanging fruit. *Curr. Opin. Struct. Biol.* **2012**, *22*, 406−412.
(11) Walker, S. I.; Packard, N.; Cody, G. D. Re-conceptualizing the origins of life. *Philos. Trans. R. Soc., A* **2017**, *375*, 20160337.
(12) Pande, V. S.; Grosberg, A. Y.; Tanaka, T. Statistical mechanics of simple models of protein folding and design. *Biophys. J.* **1997**, *73*, 3192−3210.
(13) Miller, D. W.; Dill, K. A. Ligand binding to proteins: the binding landscape model. *Protein Sci.* **1997**, *6*, 2166−2179.
(14) Eckmann, J.-P.; Rougemont, J.; Tlusty, T. *Colloquium:* Proteins: The physics of amorphous evolving matter. *Rev. Mod. Phys.* **2019**, *91*, No. 03100.
(15) Chennubhotla, C.; Rader, A. J.; Yang, L. W.; Bahar, I. Elastic network models for understanding biomolecular machinery: from enzymes to supramolecular assemblies. *Phys. Biol.* **2005**, *2*, S173−S180.
(16) Bahar, I.; Atilgan, A. R.; Erman, B. Direct evaluation of thermal fluctuations in proteins using a single-parameter harmonic potential. *Folding Des.* **1997**, *2*, 173−181.
(17) Tama, F.; Sanejouand, Y.-H. Conformational change of proteins arising from normal mode calculations. *Protein Eng., Des. Sel.* **2001**, *14*, 1−6.
(18) Dietz, H.; Rief, M. Elastic bond network model for protein unfolding mechanics. *Phys. Rev. Lett.* **2008**, *100*, No. 098101.
(19) Srivastava, A.; Granek, R. Cooperativity in thermal and force-induced protein unfolding: integration of crack propagation and network elasticity models. *Phys. Rev. Lett.* **2013**, *110*, 138101−138105.
(20) Savir, Y.; Tlusty, T. Conformational proofreading: the impact of conformational changes on the specificity of molecular recognition. *PLoS One* **2007**, *2*, e468−e468.
(21) McLeish, T. C. B.; Rodgers, T. L.; Wilson, M. R. Allostery without conformation change: modelling protein dynamics at multiple scales. *Phys. Biol.* **2013**, *10*, No. 056004.
(22) Yan, L.; Ravasio, R.; Brito, C.; Wyart, M. Architecture and coevolution of allosteric materials. *Proc. Natl. Acad. Sci. U. S. A.* **2017**, *114*, 2526−2531.
(23) Haldane, J. B. S. *Enzymes*; Green and Co: UK, 1930.
(24) Gavish, B. The role of geometry and elastic strains in dynamic states of proteins. *Biophys. Struct. Mech.* **1978**, *4*, 37−52.
(25) Gavish, B. Molecular dynamics and the transient strain model of enzyme catalysis. in *The fluctuating enzyme*; Ed. Welch, G. R. pp. 263−339, Wiley: New York, 1986.
(26) Bustamante, C.; Chemla, Y. R.; Forde, N. R.; Izhaky, D. Mechanical processes in biochemistry. *Annu. Rev. Biochem.* **2004**, *73*, 705−748.
(27) Zeravcic, Z.; Brenner, M. P. Spontaneous emergence of catalytic cycles with colloidal spheres. *Proc. Natl. Acad. Sci. U. S. A.* **2017**, *114*, 4342−4347.
(28) Cornish-Bowden, A. *Principles of enzyme kinetics*; Elsevier: 2014.
(29) Eisenthal, R.; Danson, M. J.; Hough, D. W. Catalytic efficiency and k_{cat}/K_M: a useful comparator? *Trends Biotechnol.* **2007**, *25*, 247−249.
(30) Kramers, H. A. Brownian motion in a field of force and the diffusion model of chemical reactions. *Physica* **1940**, *7*, 284−304.
(31) Pauling, L. Molecular architecture and biological reactions. *Chem. Eng. News* **1946**, *24*, 1375−1377.
(32) Lienhard, G. E. Enzymatic catalysis and transition-state theory. *Science* **1973**, *180*, 149−154.
(33) Hilvert, D. Critical analysis of antibody catalysis. *Annu. Rev. Biochem.* **2000**, *69*, 751−793.
(34) Rivoire, O. Parsimonious evolutionary scenario for the origin of allostery and coevolution patterns in proteins. *Phys. Rev. E* **2019**, *100*, No. 032411.
(35) Barato, A. C.; Seifert, U. Universal bound on the fano factor in enzyme kinetics. *J. Phys. Chem. B* **2015**, *119*, 6555−6561.
(36) Min, W.; Xie, X. S.; Bagchi, B. Two-dimensional reaction free energy surfaces of catalytic reaction: effects of protein conformational dynamics on enzyme catalysis. *J. Phys. Chem. B* **2008**, *112*, 454−466.
(37) Kohen, A.; Klinman, J. P. Enzyme catalysis: beyond classical paradigms. *Acc. Chem. Res.* **1998**, *31*, 397−404.
(38) Hemery, M.; Rivoire, O. Evolution of sparsity and modularity in a model of protein allostery. *Phys. Rev. E* **2015**, *91*, No. 042704.

https://dx.doi.org/10.1021/acs.jpcb.0c00244
J. Phys. Chem. B 2020, 124, 807−813